

# Cosmic reionization after Planck

Sourav Mitra<sup>1\*</sup>, T. Roy Choudhury<sup>2†</sup> and Andrea Ferrara<sup>3‡</sup>

<sup>1</sup>*University of the Western Cape, Bellville, Cape Town 7535, South Africa*

<sup>2</sup>*National Centre for Radio Astrophysics, TIFR, Post Bag 3, Ganeshkhind, Pune 411007, India*

<sup>3</sup>*Scuola Normale Superiore, Piazza dei Cavalieri 7, 56126 Pisa, Italy*

4 November 2018

## ABSTRACT

Cosmic reionization holds the key to understand structure formation in the Universe, and can inform us about the properties of the first sources, as their star formation efficiency and escape fraction of ionizing photons. By combining the recent release of Planck electron scattering optical depth data with observations of high-redshift quasar absorption spectra, we obtain strong constraints on viable reionization histories. We show that inclusion of Planck data favors a reionization scenario with a single stellar population. The mean  $x_{\text{HI}}$  drops from  $\sim 0.9$  at  $z = 10.6$  to  $\sim 0.02$  at  $z = 5.8$  and reionization is completed around  $5.8 \lesssim z \lesssim 9.3$  ( $2\sigma$ ), thus indicating a significant reduction in contributions to reionization from high redshift sources. We can put independent constraints on the escape fraction  $f_{\text{esc}}$  of ionizing photons by incorporating the high-redshift galaxy luminosity function data into our analysis. We find that  $f_{\text{esc}}$  increases moderately from 9% to 20% in the redshift range  $z = 6 - 9$ . Such result is however consistent at  $2\sigma$  confidence level with a non-evolving escape fraction.

**Key words:** dark ages, reionization, first stars – intergalactic medium – cosmology: theory – large-scale structure of Universe.

## 1 INTRODUCTION

Cosmic reionization is one of the key events in the history of Universe. Most of the available constraints on the epoch of reionization (EoR) come from the observations of the CMB by the Wilkinson Microwave Anisotropy Probe (WMAP) satellite (Komatsu et al. 2011; Hinshaw et al. 2013; Bennett et al. 2013), and from high redshift QSOs (Becker et al. 2001; White et al. 2003; Fan et al. 2006). The recent nine-year WMAP observations provide the value of integrated Thomson scattering optical depth  $\tau_{\text{el}} = 0.089 \pm 0.014$  (Hinshaw et al. 2013). This in turn corresponds to an instantaneous reionization taking place at redshift  $z_{\text{reion}} = 10.6 \pm 1.1$ , indicating a strong need for sources of reionization at  $z \gtrsim 10$ . However, improved measurements from three-year Planck mission suggest a lower value,  $\tau_{\text{el}} = 0.066 \pm 0.012$ , (Planck Collaboration et al. 2015) corresponding to  $z_{\text{reion}} = 8.8_{-1.1}^{+1.2}$  and therefore cuts down the demand for reionization sources beyond redshift  $z = 10$  (Robertson et al. 2015; Bouwens et al. 2015). The resulting reionization histories seem to explain the observations of Lyman- $\alpha$  emitters at  $z \sim 7$  (Mesinger et al. 2015; Choudhury et al. 2014) which were otherwise in tension with the WMAP constraints. Although, these observations of cosmological data analysis are based on the assumption that reionization is a sudden and instantaneous process, recent studies (Barkana & Loeb 2001;

Choudhury & Ferrara 2006a,b; Choudhury 2009; Pritchard et al. 2010; Mitra et al. 2011, 2012; Ghara et al. 2015) clearly support a more extended process spanning the redshift range  $6 < z < 15$ . Several semi-analytical models have been proposed with a combination of different observations to put tighter limits on the reionization redshift and other quantities related to reionization (Choudhury & Ferrara 2005; Wyithe & Loeb 2005; Gallerani et al. 2006; Dijkstra et al. 2007; Samui et al. 2007; Iliev et al. 2008; Mitra et al. 2011; Kulkarni & Choudhury 2011; Mitra et al. 2012; Cai et al. 2014).

Another observation set that could be used to check the consistency of such models is Luminosity Function (LF) of high- $z$  ( $6 \lesssim z \lesssim 10$ ) galaxies (Bouwens & Illingworth 2006; Oesch et al. 2012; Bradley et al. 2012; Oesch et al. 2014; Bowler et al. 2014; McLeod et al. 2014; Bouwens et al. 2015). This procedure has to deal with the yet poorly understood escape fraction of ionizing photons ( $f_{\text{esc}}$ ). Despite of numerous impressive efforts in both observational and theoretical studies, this quantity, as a function of galaxy mass and redshift, remains largely uncertain (Fernandez & Shull 2011). Available studies generally lead to a broad range and as well as contradictory trends of  $f_{\text{esc}}$  on redshift. For example, Finkelstein et al. (2012) estimated average  $f_{\text{esc}}$  to be  $\sim 30\%$  in order to get a fully ionized IGM at  $z = 6$ . Kuhlen & Faucher-Giguère (2012) found a strong redshift evolution of escape fraction increasing from  $\sim 4\%$  at  $z = 4$  to unity at higher redshifts in order to simultaneously satisfy reionization and lower redshift Lyman- $\alpha$  forest constraints. Based on a robust statistical analysis on full CMB spectrum and quasar data and using the obser-

\* E-mail: hisourav@gmail.com

† E-mail: tirth@ncra.tifr.res.in

‡ E-mail: andrea.ferrara@sns.it

variations of high- $z$  galaxy LFs, we (Mitra et al. 2013) derived that mean value of  $f_{\text{esc}}$  is moderately increasing from 7% at  $z = 6$  to 18% at  $z = 8$ . This increasing behavior of  $f_{\text{esc}}$  on redshift is somewhat similar to that obtained or assumed in Inoue et al. (2006); Razoumov & Sommer-Larsen (2010); Haardt & Madau (2011, 2012); Ferrara & Loeb (2013); Finlator et al. (2015). More recently, using a high-resolution cosmological zoom-in simulation of galaxy formation, Ma et al. (2015) found a considerably lower ( $< 5\%$ ; much less than required by reionization models) and a non-evolving escape fraction. This unchanging trend of  $f_{\text{esc}}$  is as well consistent with many other earlier results (Gnedin 2008; Yajima et al. 2011). A decreasing tendency of escape fraction with redshift has also been reported in the literature (Wood & Loeb 2000; Kimm & Cen 2014).

For all these reasons, here we revise our reionization models (Mitra et al. 2013) in the light of recently available Planck data and improved measurements of high- $z$  LFs<sup>1</sup>.

## 2 DATA-CONSTRAINED REIONIZATION MODEL

Let us first summarize the main features of the semi-analytical model for inhomogeneous reionization used in this analysis, which is based on Choudhury & Ferrara (2005) and Choudhury & Ferrara (2006b). The model tracks the ionization and thermal evolution of all hydrogen and helium regions separately and self-consistently by adopting a *lognormal* probability distribution (Choudhury & Ferrara 2005). The model considers the inhomogeneities in the IGM according to the description given by MHR (Miralda-Escudé et al. 2000), in which once all the low-density regions are ionized, reionization is said to be complete (see Choudhury 2009).

The sources of reionization are assumed to be stars (metal-free PopIII and normal PopII) and quasars. Furthermore, the model calculates the suppression of star formation in low-mass haloes (*radiative feedback*) through a Jeans mass prescription and accounts for the *chemical feedback* (PopIII  $\rightarrow$  PopII transition) using merger-tree based genetic approach (Schneider et al. 2006). The model computes the production rate of ionizing photons in the IGM as

$$\dot{n}_{\text{ph}}(z) = n_b N_{\text{ion}} \frac{df_{\text{coll}}}{dt} \quad (1)$$

where,  $f_{\text{coll}}$  is the collapsed fraction of dark matter halo,  $n_b$  is the total baryonic number density in the IGM and  $N_{\text{ion}}$ , possibly a function of halo mass and redshift, is the number of photons entering the IGM per baryon in stars. This quantity can be written as  $N_{\text{ion}} = \epsilon_* f_{\text{esc}} N_\gamma$ , where  $\epsilon_*$  is the star formation efficiency, and  $N_\gamma$  is the specific number of photons emitted per baryon in stars (Mitra et al. 2013):

### 2.1 MCMC-PCA constraints from Planck data

From the above model, we obtain the redshift evolution of  $N_{\text{ion}}(z)$  and other quantities by performing a detailed likelihood estimation using the Principal Component Analysis (PCA), following

Mitra et al. (2011, 2012). We assume  $N_{\text{ion}}$  as an arbitrary function of  $z$  and decompose it into its principal components by constructing the Fisher matrix from a fiducial model for  $N_{\text{ion}}$  using three different datasets: (i) measurements of photoionization rates  $\Gamma_{\text{PI}}$  in  $2.4 \leq z \leq 6$  from Bolton & Haehnelt (2007) and Becker & Bolton (2013); (ii) redshift evolution of Lyman-limit systems (LLS),  $dN_{\text{LL}}/dz$  over a wide redshift range ( $0.36 < z < 6$ ) by Songaila & Cowie (2010); (iii) Thomson scattering optical depth  $\tau_{\text{el}}$  using recent Planck data (Planck Collaboration et al. 2015). We choose the fiducial model to be constant (no redshift dependence) as it matches the above-mentioned data points quite accurately. When computing the ionizing radiation properties, we include only a single stellar population (PopII) and neglect the contributions from PopIII sources (thus no *chemical feedback* in the model) since such effects will be indirectly included in the evolution of  $N_{\text{ion}}$  itself.

We then take the first 2 – 7 PCA modes (eigen-modes of the Fisher matrix), having the largest eigenvalues or smallest uncertainties, which satisfy a model-independent Akaike information criteria (AIC; Liddle 2007) and finally perform the Markov Chain Monte Carlo (MCMC) analysis<sup>2</sup> using those modes; for details, see Mitra et al. (2011, 2012). As the Planck collaboration has not published low- $\ell$  polarization data, we include only Planck optical depth data in the analysis. However, if one may wish to include the full CMB spectra into the analysis, one should also consider variations in  $\sigma_8$  and  $n_s$  to avoid their possible degeneracies with the reionization model parameters (Pandolfi et al. 2011; Mitra et al. 2012).

The MCMC constraints on the model are shown in Fig. 1. The fiducial model is well inside the shaded regions for all redshift range. One can see that, overall our model predictions match the observed data points quite reasonably. We find that, all the quantities are tightly constrained at  $z \lesssim 6$ . This is expected as most of the observational information considered in this work exists only at those redshifts. On the other hand, a wide range of histories at  $z > 6$  is still permitted by the data. The 2- $\sigma$  confidence limits (C.L.) start to decrease at redshift  $z \gtrsim 13$  since the components of the Fisher matrix are zero and there is no significant information from the PCA modes beyond this point.

For comparison, we also show the model constrained by the WMAP9  $\tau_{\text{el}} = 0.089 \pm 0.014$  value and corresponding cosmological parameters (Hinshaw et al. 2013). The mean evolution of all the quantities for this model is almost identical to the Planck one at  $z \lesssim 6$ ; at earlier epochs they start to differ, as expected from the different e.s. optical depth. However, the mean model for WMAP9 lies within Planck's 2- $\sigma$  limits only up to  $z \lesssim 9$ . Although the mean evolution of  $N_{\text{ion}}(z)$  for Planck shows a certain increase at  $z > 6$ , a non-evolving  $N_{\text{ion}}$  is still permitted within 2- $\sigma$  C.L. This is one of the key results from this work and deserves some more insight.

Unlike the WMAP9 model, the smaller value of  $\tau_{\text{el}}$  from Planck essentially releases the need for high-redshift ionizing sources and allows the reionization to be completed from only a single stellar population (PopII). The mean evolution of photoionization rates  $\Gamma_{\text{PI}}$  shows a sudden increase at  $z > 6$  with a peak around  $z \approx 7$ . The WMAP model shows a relatively higher value of  $\Gamma_{\text{PI}}$  at early epochs as it still allows the contributions coming from PopIII stars, which are able to produce large number of ionizing photons. A similar trend is also found in the evolution of LLSs. Thus the future observations on LLS around these epochs may be able to further discriminate between these two models. From the evolu-

<sup>1</sup> Throughout this Letter, we assume a flat Universe with Planck cosmological parameters:  $\Omega_m = 0.3089$ ,  $\Omega_\Lambda = 1 - \Omega_m$ ,  $\Omega_b h^2 = 0.02230$ ,  $h = 0.6774$ ,  $\sigma_8 = 0.8159$ ,  $n_s = 0.9667$  and  $Y_p = 0.2453$  (Planck Collaboration et al. 2015).

<sup>2</sup> All cosmological parameters are fixed at their best-fit Planck value.

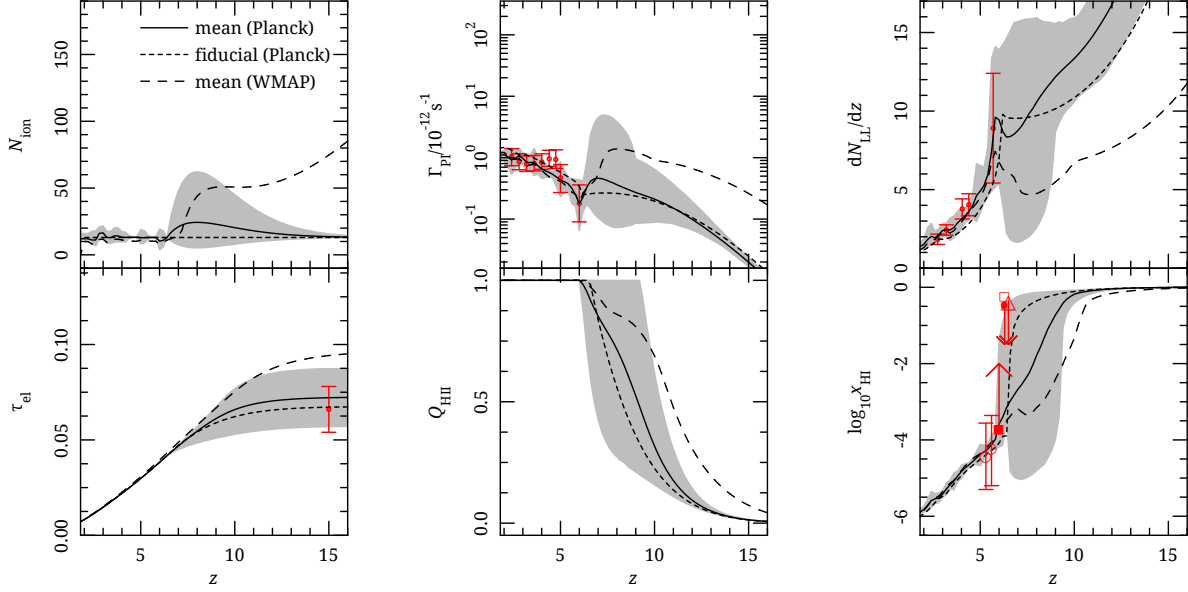


**Figure 1.** MCMC results: The mean value (solid lines) and its 2- $\sigma$  limits (shaded regions) for various quantities related to reionization obtained from our current analysis with Planck data. The fiducial model (short-dashed lines) and the model constrained using WMAP9  $\tau_{\text{eI}}$  data (long-dashed lines) also shown for comparison. The red points with errorbars that we have used to constrain the model are taken from the observations of photoionization rates  $\Gamma_{\text{PI}}$  (Bolton & Haehnelt 2007; Becker & Bolton 2013; *top-middle* panel), The redshift distribution of LLS  $dN_{\text{LL}}/dz$  (Songaila & Cowie 2010; *top-right* panel) and the recent measurements of electron scattering optical depth  $\tau_{\text{eI}}$  from Planck mission (Planck Collaboration et al. 2015; *bottom-left* panel). We also show the observational limits on neutral hydrogen fraction  $x_{\text{HI}}(z)$  (*bottom-right* panel), which we have not included in the analysis to constrain our model, from various measurements by Gallerani et al. (2008) (open circles), Fan et al. (2006) (filled square), Gallerani et al. (2008) (filled circle), Totani et al. (2006) (open square) and Kashikawa et al. (2006) (open triangle).

tion of volume filling factor  $Q_{\text{HII}}$  for HII regions, one can see that reionization is almost completed ( $Q_{\text{HII}} \sim 1$ ) around  $5.8 \lesssim z \lesssim 9.3$  (2- $\sigma$  limits) for Planck model. The mean ionized fraction evolves rapidly in  $5.8 \lesssim z \lesssim 10.6$ , in good agreement with other recent works (George et al. 2015; Robertson et al. 2015), whereas the mean WMAP model favors a relatively gradual or extended reionization (spanning  $5.8 \lesssim z \lesssim 13$ ). This is reflected in the evolution of the neutral hydrogen fraction  $x_{\text{HI}}$ : the mean value for Planck model goes from  $x_{\text{HI}} \sim 0.9$  to  $x_{\text{HI}} \sim 0.02$  between  $z = 10.6$  ( $z = 13$  for WMAP model) and  $z = 5.8$ . Overall our model prediction for  $x_{\text{HI}}(z)$  is consistent with the observational limits from from QSO absorption lines, Ly- $\alpha$  emitter (LAE) luminosity functions and GRB spectrum analysis (shown in the Fig. 1), which have not been used to constrain the model. As our Planck model seems to favor slightly higher values of  $\tau_{\text{eI}}$  than observed, a wide range of early reionization scenarios is still allowed.

### 3 UV LUMINOSITY FUNCTION

From the above data-constrained reionization models, we now derive the high- $z$  LFs, following Mitra et al. 2013. The luminosity at 1500 Å of a galaxy with mass  $M$  and age  $\Delta t$  ( $= t_z - t_{z'}$ ; time elapsed between the redshift of formation  $z'$  and redshift of observation  $z$ ) can be written as (Samui et al. 2007; Kulkarni & Choudhury 2011):

$$L_{1500}(M, \Delta t) = \epsilon_* \left( \frac{\Omega_b}{\Omega_m} \right) M l_{1500}(\Delta t) \quad (2)$$

where,  $\epsilon_*$  is the star-forming efficiency of PopII stars only as we will restrict ourselves to a single stellar population throughout this analysis. The template specific luminosity  $l_{1500}$  is computed from

stellar population synthesis model of Bruzual & Charlot (2003) for PopII stars having different metallicities in the range  $Z = 0.0001 - 0.05$ . Here we have incorporated the mass-metallicity relation given by Dayal et al. (2009) and Dayal et al. (2010) and take the appropriate model with that metallicity. The luminosity is then converted to standard absolute AB magnitude system (Oke & Gunn 1983; Kulkarni & Choudhury 2011), and finally we obtain the LF,  $\Phi(M_{\text{AB}}, z)$ , from

$$\Phi(M_{\text{AB}}, z) = \frac{dn}{dM_{\text{AB}}} = \frac{dn}{dL_{1500}} \frac{dL_{1500}}{dM_{\text{AB}}} \quad (3)$$

where  $dn/dL_{1500}$  is the comoving number of objects having luminosity within  $[L_{1500}, L_{1500} + dL_{1500}]$  at a redshift  $z$ . This quantity can be calculated from the formation rate of haloes using our reionization model (Choudhury & Ferrara 2007).

Now, we vary  $\epsilon_*$  in eq. 2 as a free parameter and match the observed LFs with our model predictions computed using eq. 3. In Fig. 2, we show our results for the best-fit  $\epsilon_*$  with 95% C.L. for redshifts  $z = 6 - 10$ . As the observations at  $z = 10$  are still scant, we are able to determine only an upper limit of  $\epsilon_*$ . The best-fit  $\epsilon_*$  remains almost constant ( $\sim 4\%$ ) for all redshift range.

Overall, the match between data and model predictions is quite impressive for all redshifts considered here. The uncertainties (shaded regions) are larger at high- $z$  and at the bright end of LFs. For lower redshifts ( $z \lesssim 7$ ), although our model can match the fainter end of the LF accurately, it slightly over-predicts the bright end. This general tendency has already been addressed in several recent works (Cai et al. 2014; Dayal et al. 2014; Bowler et al. 2014 and the references therein). In particular, Cai et al. (2014) argued that it can be resolved by taking the dust obscuration into account, which we are neglecting here. As the dust extinction was insignificant at earlier times, we are getting a good match for the

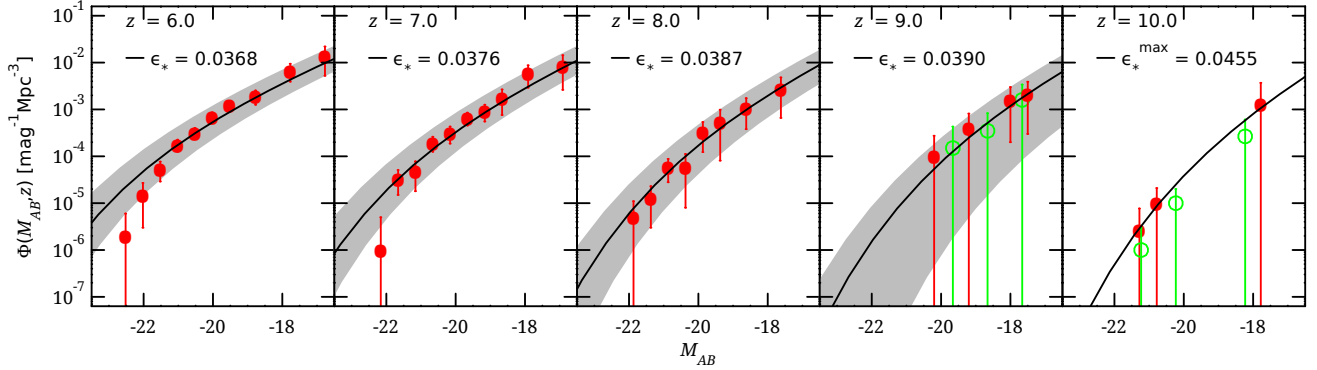


**Figure 2.** Evolution of luminosity function from our model for best-fit  $\epsilon_*$  (black curve) and 2- $\sigma$  limits (shaded region) at  $z = 6 - 10$ . Data (red) points with 2- $\sigma$  errors are: Bouwens et al. (2015) (for  $z = 6, 7, 8$ ), combined datasets from McLure et al. (2013) and McLeod et al. (2014) for  $z = 9$  and improved data from Oesch et al. (2014) for  $z = 10$ . For completeness, we also show data from Oesch et al. (2013) for  $z = 9$  and Bouwens et al. (2015) for  $z = 10$  (not included in our analysis, open green points).

Redshift	best-fit $\epsilon_*$ [2- $\sigma$ limits]	best-fit $f_{\text{esc}}$ [2- $\sigma$ limits]
$z = 6$	0.0368 [0.0189, 0.0743]	0.0872 [0.0176, 0.1761]
$z = 7$	0.0376 [0.0194, 0.0773]	0.1748 [0.0410, 0.4136]
$z = 8$	0.0387 [0.0170, 0.0764]	0.1958 [0.0489, 0.5217]
$z = 9$	0.0390 [0.0050, 0.0785]	0.1941 [0.0495, 0.5216]
$z = 10$	$< 0.0455$	$> 0.1400$

**Table 1.** Best-fit values and 2- $\sigma$  limits of star-forming efficiency  $\epsilon_*$  and the escape fraction  $f_{\text{esc}}$  obtained from the LF matching at different redshifts  $z = 6 - 10$ . At  $z = 10$ , we only get an upper limit of  $\epsilon_*$  and a corresponding lower limit of  $f_{\text{esc}}$ .

brighter end at  $z > 7$ . Alternatively, the surveyed volumes might be too small to catch the brightest, rare objects (for a discussion, see Bowler et al. 2014; Dayal et al. 2014). However, it is still unclear whether this discrepancy arises from neglecting dust or halo mass quenching (Peng et al. 2010), or it is due to a mass-dependent  $\epsilon_*$ . Thus it would be interesting to take those effects in our model which we prefer to leave for future work.

### 3.1 Escape fraction evolution

As a final step, having fixed  $\epsilon_*$  for different redshifts, we can derive limits for  $f_{\text{esc}}$  using the reionization constraints on the evolution of  $N_{\text{ion}}$  (Sec. 2.1) with  $N_{\gamma} = 3200$  as appropriate for the PopII Salpeter IMF assumed here. The uncertainties in  $f_{\text{esc}}$  can also be calculated using the quadrature method (Mitra et al. 2013). We show our resulting  $f_{\text{esc}}$  in Table 1 and Fig. 3. We find a very moderate increase of best-fit  $f_{\text{esc}}$  from  $\sim 9\%$  at  $z = 6$  to  $\sim 20\%$  at  $z = 9$ . However, the data is still consistent with a non-evolving (constant)  $f_{\text{esc}}$  within the errorbars. For  $z = 10$ , we get a lower limit of 14% which is a very strong constraint given the uncertainties present in high- $z$  observations.

## 4 CONCLUSIONS

Over the past few years, several numerical and analytical approaches have tried to constrain reionization scenarios by using CMB WMAP observations and QSOs. In particular, in our earlier works (Mitra et al. 2011, 2012), we proposed a detailed semi-analytical modeling of hydrogen reionization using the observa-

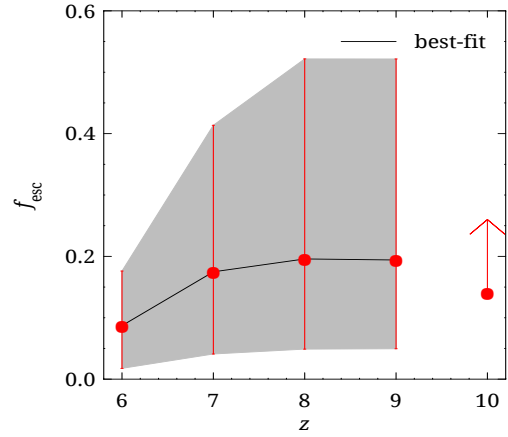


**Figure 3.** Redshift evolution of the escape fraction  $f_{\text{esc}}$  with 2- $\sigma$  errors. The  $z = 10$  point shows the lower limit on  $f_{\text{esc}}$  at that redshift.

tions for photoionization rates, redshift evolution of LLS and CMB and succeeded to produce a good match with a variety of other relevant datasets. We further tested the model against the observations of luminosity functions from high-redshift galaxies (Mitra et al. 2013). In this Letter, we extend those works by taking the recently published  $\tau_{\text{el}}$  data from Planck Collaboration et al. (2015) and various new results from the observations of galaxy LFs at  $6 \leq z \leq 10$ .

- We find that, contrary to WMAP data, a constant/non-evolving  $N_{\text{ion}}$  is now allowed by the Planck data. This immediately tells us that, reionization with a single stellar population (PopII) or non-evolving IMF is possible, i.e. the impact of PopIII stars on reionization (Paardekooper et al. 2013) is likely to be negligible.

- According to Planck data, reionization proceeds quickly from  $z \approx 10.6$  to  $z \approx 5.8$  as the mean  $x_{\text{HI}}$  drops from 0.9 to 0.02 within these epochs. We find that reionization is almost completed around  $5.8 \lesssim z \lesssim 9.3$  (2- $\sigma$  C.L.). However, the model with WMAP data seems to favor an extended reionization starting as early as  $z \approx 13$ . Thus, the inclusion of Planck data in turn indicates that most of the reionization activity occurs at  $z \lesssim 10$  (Robertson et al. 2015; Bouwens et al. 2015).

- From the match between the observed high-redshift LFs and our model predictions, we find that the best-fit values for both  $\epsilon_*$  and  $f_{\text{esc}}$  increase very moderately with redshifts:  $\epsilon_*$  remains con-

stant at  $\sim 4\%$ ;  $f_{\text{esc}}$  increases from  $\sim 9\%$  at  $z = 6$  to  $\sim 20\%$  at  $z = 9$ . Such result is however consistent at  $2\text{-}\sigma$  confidence level with a non-evolving escape fraction (Gnedin 2008; Yajima et al. 2011; Ma et al. 2015). We have also obtained the tightest constraint available to our knowledge on  $f_{\text{esc}}$  ( $> 14\%$ ) at  $z = 10$ .

Although we have focused on high-redshift LFs, one can apply the same method for the evolution in lower redshift range  $3 \leq z \leq 5$ . As the dust extinction becomes significant at those redshifts, one has to take that into account. Moreover, the addition of dust and/or a mass-dependent  $\epsilon_*$  may resolve the problem of overproducing the brighter end of LFs, as stated earlier. We defer these issues to future work. Also, the inclusion of *full* CMB datasets from Planck into our analysis can be helpful for ruling out some of the current reionization scenarios. Unfortunately, the recent Planck data release does not include the polarization data in their likelihood; instead, they rely on the WMAP polarization likelihood at low multipoles (Planck Collaboration et al. 2015). As most of the constraints at  $z > 6$  related to reionization models come from polarization data (Mitra et al. 2012), we postpone such analysis to the next Planck data release.

## REFERENCES

- Barkana R., Loeb A., 2001, *Phys. Rep.*, 349, 125
- Becker G. D., Bolton J. S., 2013, *MNRAS*, 436, 1023
- Becker R. H., et al., 2001, *Astron.J.*, 122, 2850
- Bennett C. L., et al., 2013, *ApJS*, 208, 20
- Bolton J. S., Haehnelt M. G., 2007, *MNRAS*, 382, 325
- Bouwens R., Illingworth G., 2006, *New Astronomy Reviews*, 50, 152
- Bouwens R. J., et al., 2015, *ApJ*, 803, 34
- Bouwens R. J., Illingworth G. D., Oesch P. A., Caruana J., Holwerda B., Smit R., Wilkins S., 2015, *arXiv:1503.08228*
- Bowler R. A. A., Dunlop J. S., McLure R. J., McCracken H. J., Furusawa H., Taniguchi Y., Fynbo J. P. U., Milvang-Jensen B., Le Fevre O., 2014, *arXiv:1411.2976*
- Bradley L. D., et al., 2012, *ApJ*, 760, 108
- Bruzual G., Charlot S., 2003, *MNRAS*, 344, 1000
- Cai Z.-Y., Lapi A., Bressan A., De Zotti G., Negrello M., Danese L., 2014, *ApJ*, 785, 65
- Choudhury T. R., 2009, *Current Science*, 97, 841
- Choudhury T. R., Ferrara A., 2005, *MNRAS*, 361, 577
- Choudhury T. R., Ferrara A., 2006a, *arXiv:astro-ph/0603149*
- Choudhury T. R., Ferrara A., 2006b, *MNRAS*, 371, L55
- Choudhury T. R., Ferrara A., 2007, *MNRAS*, 380, L6
- Choudhury T. R., Puchwein E., Haehnelt M. G., Bolton J. S., 2014, *arXiv:1412.4790*
- Dayal P., Ferrara A., Dunlop J. S., Pacucci F., 2014, *MNRAS*, 445, 2545
- Dayal P., Ferrara A., Saro A., 2010, *MNRAS*, 402, 1449
- Dayal P., Ferrara A., Saro A., Salvaterra R., Borgani S., Tornatore L., 2009, *MNRAS*, 400, 2000
- Dijkstra M., Wyithe J. S. B., Haiman Z., 2007, *MNRAS*, 379, 253
- Fan X., et al., 2006, *AJ*, 132, 117
- Fernandez E. R., Shull J. M., 2011, *ApJ*, 731, 20
- Ferrara A., Loeb A., 2013, *MNRAS*, 431, 2826
- Finkelstein S. L., et al., 2012, *ApJ*, 758, 93
- Finlator K., Thompson R., Huang S., Davé R., Zackrisson E., Oppenheimer B. D., 2015, *MNRAS*, 447, 2526
- Gallerani S., Choudhury T. R., Ferrara A., 2006, *MNRAS*, 370, 1401
- Gallerani S., Ferrara A., Fan X., Choudhury T. R., 2008, *MNRAS*, 386, 359
- Gallerani S., Salvaterra R., Ferrara A., Choudhury T. R., 2008, *MNRAS*, 388, L84
- George E. M., et al., 2015, *ApJ*, 799, 177
- Ghara R., Datta K. K., Choudhury T. R., 2015, *arXiv:1504.05601*
- Gnedin N. Y., 2008, *ApJL*, 673, L1
- Haardt F., Madau P., 2011, *arXiv:1103.5226*
- Haardt F., Madau P., 2012, *ApJ*, 746, 125
- Hinshaw G., et al., 2013, *ApJS*, 208, 19
- Iliev I. T., Shapiro P. R., McDonald P., Mellema G., Pen U.-L., 2008, *MNRAS*, 391, 63
- Inoue A. K., Iwata I., Deharveng J.-M., 2006, *MNRAS*, 371, L1
- Kashikawa N., et al., 2006, *ApJ*, 648, 7
- Kimm T., Cen R., 2014, *ApJ*, 788, 121
- Komatsu E., et al., 2011, *Astrophys.J.Suppl.*, 192, 18
- Kuhlen M., Faucher-Giguère C.-A., 2012, *MNRAS*, 423, 862
- Kulkarni G., Choudhury T. R., 2011, *MNRAS*, 412, 2781
- Liddle A. R., 2007, *MNRAS*, 377, L74
- Ma X., Kasen D., Hopkins P. F., Faucher-Giguère C.-A., Quataert E., Keres D., Murray N., 2015, *arXiv:1503.07880*
- McLeod D. J., McLure R. J., Dunlop J. S., Robertson B. E., Ellis R. S., Targett T. T., 2014, *arXiv:1412.1472*
- McLure R. J., et al., 2013, *MNRAS*, 432, 2696
- Mesinger A., Aykatalp A., Vanzella E., Pentericci L., Ferrara A., Dijkstra M., 2015, *MNRAS*, 446, 566
- Miralda-Escudé J., Haehnelt M., Rees M. J., 2000, *ApJ*, 530, 1
- Mitra S., Choudhury T. R., Ferrara A., 2011, *MNRAS*, 413, 1569
- Mitra S., Choudhury T. R., Ferrara A., 2012, *MNRAS*, 419, 1480
- Mitra S., Ferrara A., Choudhury T. R., 2013, *MNRAS*, 428, L1
- Oesch P. A., et al., 2012, *ApJ*, 745, 110
- Oesch P. A., et al., 2013, *ApJ*, 773, 75
- Oesch P. A., et al., 2014, *ApJ*, 786, 108
- Oke J. B., Gunn J. E., 1983, *ApJ*, 266, 713
- Paardekooper J.-P., Khochfar S., Dalla Vecchia C., 2013, *MNRAS*, 429, L94
- Pandolfi S., Ferrara A., Choudhury T. R., Melchiorri A., Mitra S., 2011, *Phys. Rev. D*, 84, 123522
- Peng Y.-j., et al., 2010, *ApJ*, 721, 193
- Planck Collaboration et al., 2015, *arXiv:1502.01589*
- Pritchard J. R., Loeb A., Wyithe J. S. B., 2010, *MNRAS*, 408, 57
- Razoumov A. O., Sommer-Larsen J., 2010, *ApJ*, 710, 1239
- Robertson B. E., Ellis R. S., Furlanetto S. R., Dunlop J. S., 2015, *ApJL*, 802, L19
- Samui S., Srianand R., Subramanian K., 2007, *MNRAS*, 377, 285
- Schneider R., Salvaterra R., Ferrara A., Ciardi B., 2006, *MNRAS*, 369, 825
- Songaila A., Cowie L. L., 2010, *ApJ*, 721, 1448
- Totani T., Kawai N., Kosugi G., Aoki K., Yamada T., Iye M., Ohta K., Hattori T., 2006, *Pub. Astron. Soc. Japan*, 58, 485
- White R. L., Becker R. H., Fan X., Strauss M. A., 2003, *AJ*, 126, 1
- Wood K., Loeb A., 2000, *ApJ*, 545, 86
- Wyithe J. S. B., Loeb A., 2005, *ApJ*, 625, 1
- Yajima H., Choi J.-H., Nagamine K., 2011, *MNRAS*, 412, 411